

LDA+DMFT study for $\text{La}_{1-x}\text{Sr}_x\text{TiO}_3$

M. B. Zölf, Th. Pruschke, J. Keller

Institut für Theoretische Physik I, Universität Regensburg, Universitätsstr. 31, 93053 Regensburg, Germany

A. I. Poteryaev, I. A. Nekrasov, V. I. Anisimov

Institute for Metal Physics, 620014 Ekaterinburg, Russia

(October 30, 2013)

The dynamical mean-field theory together with the non-crossing approximation is used to set up a novel scheme to study the electronic structure of strongly correlated electron systems. The non-interacting band structure is obtained from a density functional calculation within the local density approximation. With this method the doped Mott insulator $\text{La}_{1-x}\text{Sr}_x\text{TiO}_3$ is studied. Starting from first-principle calculations for a cubic and an orthorhombic system we determined the one-particle spectrum. Both one-particle spectra show a lower Hubbard band (seen as $d^1 \rightarrow d^0$ transitions in photoemission experiments), a Kondo resonance near the Fermi energy and the upper Hubbard band ($d^1 \rightarrow d^2$ transitions in an inverse photoemission experiment). The upper Hubbard band develops a multipeak structure, a consequence of the consideration of all local two-particle correlations, which leads to the full multiplet structure in the atomic limit. The calculation for the orthorhombic system shows qualitative good agreement when compared with experimental photoemission spectra.

71.27.+a Strongly correlated electron systems , 71.30.+h Metal-insulator transitions and other electronic transitions , 74.25.Jb Electronic structure

I. INTRODUCTION

One of the most challenging problems in condensed-matter physics is the accurate calculation of the electronic structure starting from first principles, since it is impossible to solve the many-body problem without severe approximations. A great success in first principle methods was the development of the density functional theory (DFT)¹, which produces an exact groundstate energy and maps the many-body problem onto a fictitious single-electron problem with an one-electron exchange and correlation potential. The method would be exact, if one knew this particular potential.

A commonly used approximation replaces this functional by the one of the homogeneous electron gas. This approximation is widely known as the local (spin-) density approximation (L(S)DA)¹. The LDA turns out to be very crude, if the on-site Coulomb interaction between electrons becomes very strong, i.e. if the interaction strength is of the order of, or larger than the bandwidth. This is particular the case in systems with d - or f -electrons. As is well known, the L(S)DA approximation leads to wrong results for strongly correlated electron systems such as Mott-Hubbard insulators or heavy

fermion systems.

A first step towards a better description of strongly correlated systems was the introduction of the LDA+U method², a Hartree-Fock-like scheme, that is able to account for a variety of interesting effects in transition metal compounds. For example, the LDA+U allows to describe correctly the groundstates of magnetically, charge and orbitally ordered materials³. Due to its Hartree-Fock nature, however, this approximation still has severe drawbacks.

To go beyond LDA+U, a new scheme was recently proposed⁴, which combines the LDA bandstructure calculation with the dynamical mean-field theory (DMFT: for a review see reference 5). The DMFT maps the lattice model onto an effective impurity problem and can be used to solve the many-body problem self-consistently with various methods, like e.g. quantum Monte Carlo (QMC)⁶, exact diagonalization (ED)⁷, iterated perturbation theory (IPT)⁸ or within the non-crossing approximation (NCA)⁹.

A calculation scheme for LDA+DMFT in conjunction with IPT was already accomplished in reference 4. However, in this work only one mean Coulomb parameter U was used to describe all local correlations. It is however well known that the complexity of the physics observed in e.g. transition metal oxides is governed by the subtle interplay of the various local Coulomb integrals, i.e. the neglect of the detailed orbital structure presents a serious limitation of the method.

In this paper a LDA+DMFT approach with the NCA is introduced, which allows to consider the full local multiplet structure. Thus, an intra orbital Coulomb energy U , an inter-orbital Coulomb energy U' , and Hund's coupling constant J are considered within a $\text{SU}(N)$ invariant formulation of the local Hamiltonian for degenerated bands¹⁰. The bandstructure calculations as starting point for the DMFT were done with the linearized muffin-tin orbital method (LMTO)¹¹. The paper is organised as follows. In section II we introduce the Hamiltonian used for the many-body calculation and describe the details of the NCA scheme used to solve the local problem. Results for $\text{La}_{1-x}\text{Sr}_x\text{TiO}_3$ as a particularly interesting example of a correlated metal obtained with this technique are collected in section III and a summary in section IV will conclude the paper.

II. THE CALCULATING SCHEME

In order to combine the achievements of the DMFT with the framework of DFT, one needs a calculation scheme that allows to map the calculated band structure onto a suitable tight-binding model. This can be done most conveniently with the LMTO in the orthogonal approximation¹¹. With this technique a tight-binding model can naturally be constructed from the DFT+LDA bands in real-space representation

$$H_{tb} = \sum_{ilm, jl'm', \sigma} (\delta_{ilm, jl'm'} \epsilon_{il} \hat{n}_{ilm\sigma} + t_{ilm, jl'm'} \hat{c}_{ilm\sigma}^\dagger \hat{c}_{jl'm'\sigma}) . \quad (1)$$

Since the LDA one-electron potential is orbital independent and takes into account the Coulomb interaction in an averaged way, one can easily generalize this Hamiltonian by adding local Coulomb correlations:

$$H_{corr} = \frac{1}{2} \sum_{il, m\sigma m'\sigma'}' U_{mm'}^{il} \hat{n}_{ilm\sigma} \hat{n}_{ilm'\sigma'} \quad (2)$$

$$+ \frac{1}{2} \sum_{il, m\sigma m'\sigma' n\rho n'\rho'}' J_{m\sigma m'\sigma' n\rho n'\rho'}^{il} \hat{c}_{ilm\sigma}^\dagger \hat{c}_{ilm'\sigma'}^\dagger \hat{c}_{iln\rho} \hat{c}_{iln'\rho'} . \quad (3)$$

In term (2) and (3), the index i labels the unit cell, l denotes the atom in the unit cell and $m\sigma$ and others stand for orbital and spin. The prime on the sum indicates that at least two of the indices on different operators have to be different to account for Pauli's principle. In our approach we are able to include all local two-particle correlations appearing in term (2) and (3). In the following we will assume, that it is only necessary to take into account the Coulomb interactions for the d -shell of the transition metal ions ($i = i_d$ and $l = l_d$) explicitly. Therefore the indices il will be omitted. All other orbitals will be considered as itinerant bands, which are well described by the LDA.

Let us discuss the interaction term in more detail. The first term (2) describes the density-density Coulomb repulsion. Here, we introduce two distinct Coulomb parameters: the intra-orbital Coulomb energy U has to be considered in case of a doubly occupied orbital, while the inter-orbital Coulomb energy U' applies for example in the case of a doubly occupied d -shell with electrons on d -orbitals with different indices. The second term (3) describes Hund's coupling and all other off-diagonal interactions. Although in principle the full Coulomb matrix (2) and (3) can be used, we restrict ourselves for practical purposes to the following, commonly used form for the two-particle interactions of the d -electrons

$$H_{corr} = U \sum_m \hat{n}_{m\uparrow} \hat{n}_{m\downarrow} + \frac{U'}{2} \sum_{m, m', \sigma, \sigma'}^{m \neq m'} \hat{n}_{m\sigma} \hat{n}_{m'\sigma'} \quad (4)$$

$$- \frac{J}{2} \sum_{m, m', \sigma}^{m \neq m'} \hat{n}_{m\sigma} \hat{n}_{m'\sigma} + J \sum_{m, m'}^{m \neq m'} c_{m\uparrow}^\dagger c_{m'\downarrow}^\dagger c_{m\downarrow} c_{m'\uparrow} \quad (5)$$

$$+ J_C \sum_{m, m'}^{m \neq m'} c_{m\uparrow}^\dagger c_{m\downarrow}^\dagger c_{m'\downarrow} c_{m'\uparrow}, \quad (6)$$

with a density-like Coulomb term (4), a SU(2)-invariant form of Hund's Coupling (5) and a charge-flip term or pair-hopping term (6). $J_C = J$ is chosen here as a good approximation.

Since the LDA already contains the influence of the Coulomb interaction to a certain degree, the problem of double counting of these contributions by using H_{corr} arises. In order to avoid this double counting one has to subtract off the interaction contributions from the LDA. Unfortunately, the precise form for one particular set of orbitals is not known and the best one can do is to account for these contributions in an averaged way. Since the LDA total energy is to a good approximation a function of the total number of electrons, one can assume that the interaction contributions have the form

$$E_I = \frac{1}{2} \bar{U} n_d (n_d - 1) - \frac{1}{2} J \sum_{\sigma} n_{d,\sigma} (n_{d,\sigma} - 1) . \quad (7)$$

Here, \bar{U} is the mean value for the Coulomb interaction and may be obtained from a first-principle calculation¹² or from experiment, for example high-energy spectroscopy. n_d is the total number of d -electrons and $n_{d,\sigma}$ is the number of d -electrons with spin σ . Distinguishing intra- and inter-orbital interaction for a N_{deg} -fold degenerate orbital-system one can determine U and U' by the relation

$$\bar{U} = \frac{U + 2(N_{deg} - 1)U'}{2N_{deg} - 1} . \quad (8)$$

Starting from given values for \bar{U} and J and using the relation $U = U' + 2J$, which is a consequence of the rotational invariance of the Hamiltonian¹⁰, one is able to determine the intra- and inter-orbital Coulomb interaction U and U' . Finally, only an expression for the local energy of the d -states is needed. In the spirit of L(S)DA+U we can define such a one-electron energy by

$$\varepsilon_d^0 = \frac{d}{dn_{d\sigma}} (E_{LDA} - E_I) \quad (9)$$

$$= \varepsilon_d^{LDA} - \bar{U} (n_d - \frac{1}{2}) + \frac{J}{2} (n_d - 1) \quad (10)$$

$$= \varepsilon_d^{LDA} - \frac{U + 2(N_{deg} - 1)U'}{2N_{deg} - 1} (n_d - \frac{1}{2})$$

$$+ \frac{J}{2} (n_d - 1), \quad (10)$$

with

$$\varepsilon_d^{LDA} = \frac{d}{dn_{d\sigma}} E_{LDA} \quad (11)$$

and E_{LDA} the total energy as calculated from DFT+LDA. With the corrected total energy functional $E_{LDA} - E_I$ one has to construct the tight-binding Hamiltonian within the framework of the LMTO-method¹¹.

Given the band structure we are now in the position to set up the scheme necessary for the DMFT. First, let us define the non-interacting Green function

$$G_\sigma^0(z) = \int d\omega \frac{\rho_\sigma^0(\omega)}{z - \omega} \quad (12)$$

via the Hilbert transform of the spectral function $\rho_\sigma^0(\omega)$ obtained from the Hamiltonian (1). Note that in general $\rho_\sigma^0(\omega)$ and consequently $G_\sigma^0(z)$ will be matrices in orbital space. The most important feature of the DMFT is that the proper one-particle self energy due to the local Coulomb interaction is purely local⁵. Thus, we obtain as an expression for the full Green function of the interacting system

$$G_\sigma(z) = G_\sigma^0(z - \Sigma(z)) = \int d\omega \frac{\rho_{d\sigma}^0(\omega)}{z - \Sigma_\sigma(z) - \omega} . \quad (13)$$

This equation must again be read as a matrix relation in orbital space. In the spirit of the DMFT⁵ eq. (13) can be cast into the form

$$G_\sigma(z) = \frac{1}{z - \varepsilon_d^0 - \Sigma_\sigma(z) - \Delta_\sigma(z)} \quad (14)$$

where a so-called hybridization function was introduced, which fulfills the standard relation

$$\lim_{\omega \rightarrow \pm\infty} \Re\{\Delta_\sigma(\omega + i\delta)\} = 0 . \quad (15)$$

The one-electron energy ε_d^0 , the imaginary part of the hybridization function and the local Coulomb parameters define a multi-orbital impurity model, which has to be solved to obtain the selfenergy $\Sigma_\sigma(z)$. Finally, eqs. (13), (14) and the solution of this impurity model define a self-consistency cycle for the solution of the lattice model within the DMFT.

In the following we will set up a resolvent perturbation theory for the multi-orbital impurity model defined above. Within this approach the model is solved approximately by considering the lowest order diagrams only, which is the well-known NCA⁹. To this end we first have to diagonalize the local Hamiltonian

$$H_{loc} = \sum_\alpha E_\alpha |\alpha\rangle\langle\alpha| \quad (16)$$

and use the basis states $\{|\alpha\rangle\}$ in the further procedure. As a consequence, all local interactions are fully included in these impurity states. Therefore, all types of local interaction terms can in principle be considered leading to a realistic multiplet structure in the atomic limit. To account for the hybridization term, we have to express the fermionic creation and annihilation operators for the d -orbitals in terms of our basis $\{|\alpha\rangle\}$, i.e.

$$d_{\kappa\sigma}^\dagger = \sum_{\alpha,\beta} D_{\beta\alpha}^{\kappa\sigma*} |\alpha\rangle\langle\beta| , \quad (17)$$

$$d_{\kappa\sigma} = \sum_{\alpha,\beta} D_{\alpha\beta}^{\kappa\sigma} |\alpha\rangle\langle\beta| , \quad (18)$$

with κ the orbital index and σ for the spin. With (17) and (18) one can straightforwardly formulate the NCA equations⁹ as

$$R_\alpha(z) = R_\alpha^0(z) + R_\alpha^o(z) \Sigma_\alpha(z) R_\alpha(z) , \quad (19)$$

with

$$R_\alpha^0(z) = \frac{1}{z - E_\alpha} , \quad (20)$$

$$\Sigma_\alpha(z) = -\frac{1}{\pi} \sum_\sigma \sum_{\kappa\kappa'} \sum_{\alpha'} \int d\varepsilon$$

$$\Im m\{\Delta_\sigma^{\kappa\kappa'}(\varepsilon)\} D_{\alpha,\alpha'}^{\kappa\sigma*} D_{\alpha',\alpha'}^{\kappa'\sigma} f(\eta_{\alpha\alpha'}\varepsilon) R_{\alpha'}(z + \eta_{\alpha\alpha'}\varepsilon) . \quad (21)$$

$f(\epsilon)$ is the Fermi function and $\eta_{\alpha\alpha'}$ is equal to 1 or -1 depending on whether one has to add or subtract an electron to excite the impurity from state $|\alpha\rangle$ to state $|\alpha'\rangle$. Again, eqs. (19)-(21) have to be solved self-consistently. Finally, we are able to calculate the d -Green function from

$$G_\sigma^{\kappa\kappa'}(i\omega) = \frac{1}{Z} \sum_{\alpha,\alpha'} D_{\alpha\alpha'}^{\kappa\sigma*} D_{\alpha\alpha'}^{\kappa'\sigma} \oint dz \frac{e^{-\beta z}}{2\pi i} R_\alpha(z) R_{\alpha'}(z + i\omega) . \quad (22)$$

In eq. (22), $Z = \sum_\alpha \oint \frac{dz e^{-\beta z}}{2\pi i} R_\alpha(z)$ denotes the impurity partition function and β is the inverse temperature.

The solution eq. (22) of the impurity problem closes the cycle (13) and (14): Starting from an initial guess for the selfenergy $\Sigma_\sigma(z)$ one obtains from eq. (14) the hybridization function $\Delta_\sigma(z)$, which is inserted into the NCA (21). From the impurity Green function (22) and the hybridization function one can then calculate a new self energy from eq. (14) and repeats the procedure until self consistency is reached.

III. RESULTS FOR $\text{La}_{1-x}\text{Sr}_x\text{TiO}_3$

We applied the procedure discussed in the previous section to $\text{La}_{1-x}\text{Sr}_x\text{TiO}_3$. This material is at high temperatures a paramagnetic metal for the undoped case ($x=0$) and becomes an antiferromagnetic insulator below $T_N = 125\text{K}$ with a very small gap of 0.2eV . Doping with a few percent of Sr leads to a paramagnetic metal with a large effective mass¹⁵. As photoemission experiments show, $\text{La}_{1-x}\text{Sr}_x\text{TiO}_3$ may be regarded as an example of a strongly correlated metal, i.e. the density of states is that of a doped Mott-Hubbard insulator.

The LaTiO_3 crystal is a slightly distorted cubic perovskite. The octahedral coordination of the oxygen ions leads to a t_{2g} - e_g crystal-field splitting, such that both bands t_{2g} and e_g are well separated, as can be seen in a standard LDA calculation (LMTO method). At the Fermi level one finds the t_{2g} band of the Ti $3d$ states. 3eV above the Fermi level and well separated from the t_{2g} band the e_g band is located. Lead by these results we can restrict ourselves to the 3-fold degenerate t_{2g} orbitals as relevant for the low temperature properties.

The Coulomb parameters $\bar{U} = 4\text{eV}$, $J = 0.6\text{eV}$ we use for the DMFT calculation were obtained from a constraint LDA calculation¹². \bar{U} was determined in a calculation, where all electrons except t_{2g} ones can screen the Coulomb interaction. (The influence of the e_g electrons on the Coulomb interaction inside t_{2g} subshell was investigated in^{13,14}). In order to show the effect of varying the Coulomb parameter on the results we chose $\bar{U} = 6\text{eV}$ in the first parameter sets, which refers to the case where e_g -electrons do not participate in the screening.

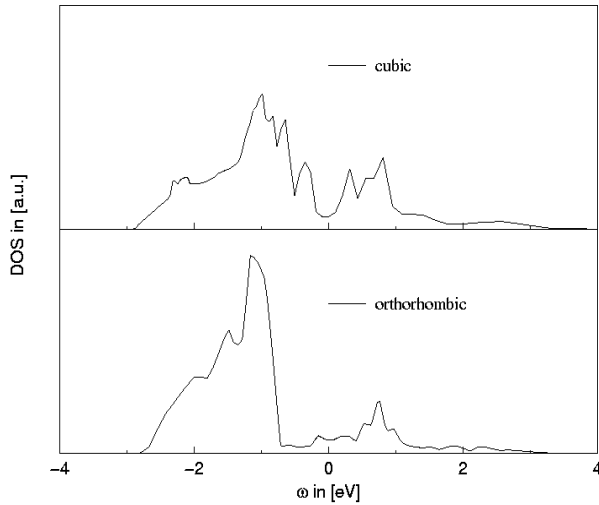


FIG. 1. The non-interacting density of states for LaTiO_3 corrected according to eq. (7) with $\bar{U} = 6\text{eV}$, $J = 0.6\text{eV}$. The upper part shows the density for a cubic, the lower part for an orthorhombic system.

In figure 1 we show the non-interacting density of states for the t_{2g} bands only taken from a LDA calculation for a cubic (upper part of figure 1) and a orthorhombic system (lower part of 1). Both spectra are corrected according to eq. (7). From the DOS in figure 1 we can determine the one-particle energy $\epsilon_{t_{2g}}^0$ as average energy, and the hybridization function $\Delta_{t_{2g}}(\omega)$ is then defined by equation (13) and (14). In figure 1 the bandwidth determined by the main contributions of the spectrum is varying for different underlying structures examined by the LDA calculation. The orthorhombic system leads to a narrower spectrum with the main contribution below the Fermi energy. The spectrum for the cubic system is broader and the spectral weight is spread over the whole

range of the band. As a consequence, the average energy of the orthorhombic system is lower than for the cubic, which leads to different one-particle energies in the resulting impurity model. It is evident that this change of bandwidth and of one-particle energy will eventually lead to different physics for both systems.

A particularly important simplification arises from the fact that the tight-binding Hamiltonian (1) constructed from the corrected LDA t_{2g} bands turns out to be diagonal in orbital space. This means that all orbital matrices in eqs. (13), (14), (21) and (22) are diagonal and – since we do not allow for orbital ordering – degenerate with respect to the orbital indices, which results in a tremendous reduction of the necessary computational effort.

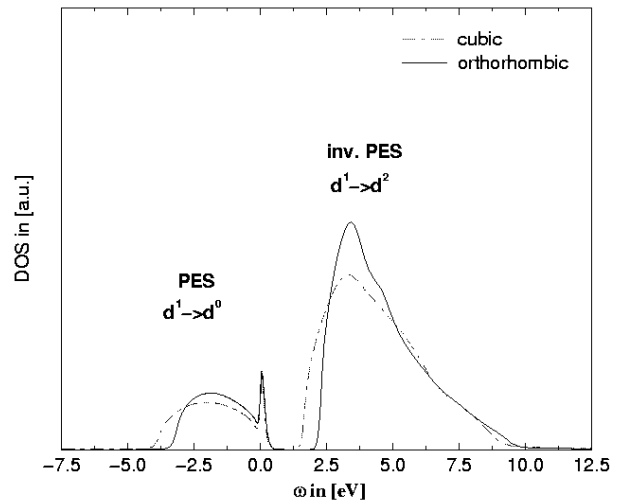


FIG. 2. t_{2g} density of states for $\text{La}_{1-x}\text{Sr}_x\text{TiO}_3$ for cubic and orthorhombic crystal structure. The parameters are: $\bar{U} = 6\text{eV}$ and $J = 0.6\text{eV}$, a reciprocal temperature $\beta = 100 \text{ eV}^{-1}$ and a doping of $x = 6\%$. The denoted transitions are the removal of electron from a single occupied t_{2g} -state and the addition of an electron to a doubly occupied state.

The results of the self-consistent DMFT calculation for the t_{2g} spectral function of a cubic and a orthorhombic system with a partially screened mean Coulomb interaction of $\bar{U} = 6\text{eV}$ and $J = 0.6\text{eV}$ and a reciprocal temperature $\beta = 100 \text{ eV}^{-1}$ are shown in figure 2. The doping level was set to $x = 6\%$. Both systems lead to qualitatively similar spectra. Especially the lower Hubbard band reaches from low energies up to the Fermi level. This band refers to $d^1 \rightarrow d^0$ transitions in a photoemission experiment. At the Fermi energy the well known many-body resonance can be seen, which describes singlet-triplet excitations of the impurity and the surrounding effective medium¹⁶. At higher energies the upper Hubbard band occurs which refers to $d^1 \rightarrow d^2$ transitions in an inverse photoemission experiment. Here contributions, which stem from transitions into several multiplet states, are almost completely smeared out to a broad, featureless band. Apart

from these gross features, the spectra show clear differences between orthorhombic and cubic system. Especially the influence of different bandwidth is clearly visible, the narrower non-interacting spectrum for the orthorhombic system leading to narrower peaks in the DMFT spectrum. As a consequence, the value of the gap between lower and upper Hubbard band is increased, too. Let us stress that the value of the gap, due to the complex atomic multiplet structure, is not simply given by the pure Coulomb interaction \bar{U} . For a partially screened mean Coulomb value of $\bar{U} = 6\text{eV}$ the real Coulomb parameters are $U = 6.96\text{eV}$ and $U' = 5.76\text{eV}$. Thus the lowest lying excitation is into a spin $S = 1$ state with an excitation energy of $\epsilon_{t_{2g}}^0 - (U' - J)$. This would lead to a gap value of 5.16eV minus bandwidth. The smaller bandwidth of the orthorhombic system thus turns out to produce an overall larger gap.

In order to exploit the difference of the value, and hence the impact of the procedure to determine \bar{U} , we compare the previous results to a calculation where a fully screened mean Coulomb energy of $\bar{U} = 4\text{eV}$ is used (i.e. $U = 4.96\text{eV}$ and $U' = 3.76\text{eV}$). Note that the value of J is not changed by using different screening scenarios, which reflects the well-known fact that the exchange coupling is rather insensitive to the detailed orbital structure and chemical surrounding in transition metal oxides.

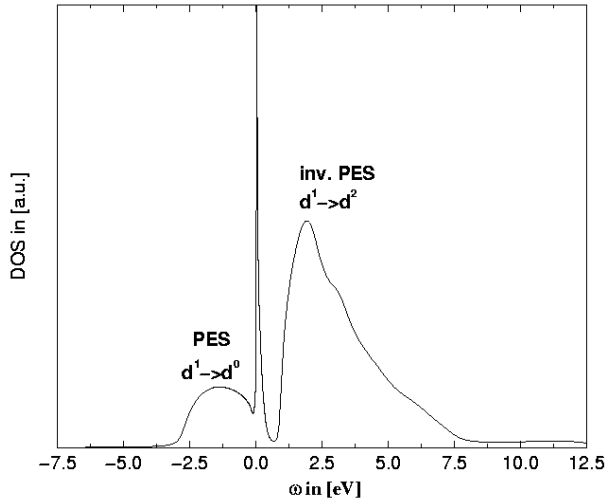


FIG. 3. The t_{2g} density of states for LaTiO_3 for the orthorhombic structure and $\bar{U} = 4\text{eV}$ and $J = 0.6\text{eV}$ at a reciprocal temperature $\beta = 100 \text{ eV}^{-1}$.

The result of the LDA+DMFT calculation for the orthorhombic system is shown in figure 3. The lowest energy difference between d^1 and d^2 is now reduced by 2eV leading to a total shift of the upper Hubbard band compared with figure 2. The multiplet structure is not affected since it is proportional to the coupling constant J only. For this set of parameters at a doping of $x = 6\%$ the lower and the upper Hubbard band is shifted towards the Fermi energy as a consequence of the smaller Coulomb

interaction compared to the partially screened case. The Kondo resonance is enlarged as a fact of different one-electron energy, which is the lowest for the orthorhombic set and for the full screened Coulomb energy \bar{U} .

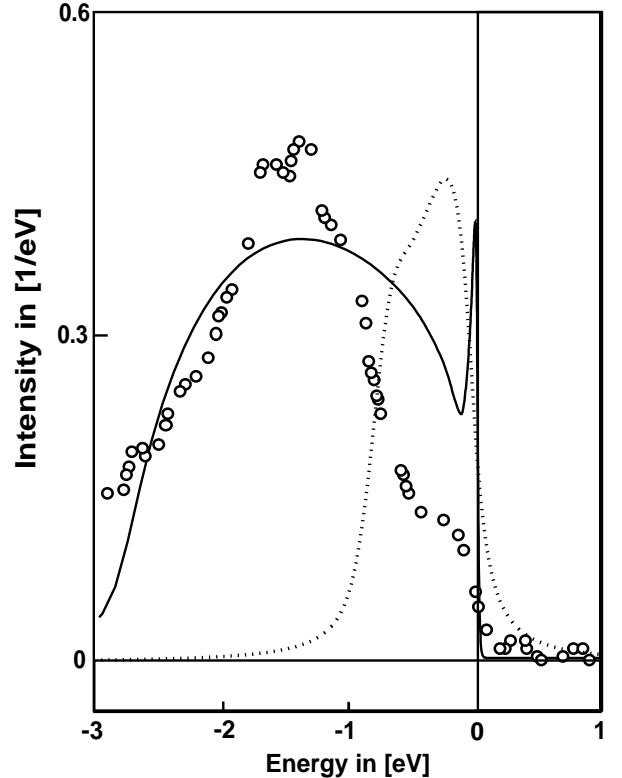


FIG. 4. The t_{2g} density of states for LaTiO_3 for orthorhombic structure given by the LDA+DMFT calculation (full line) compared with LDA results (dotted curve) and data points from a photoemission experiment for $\text{La}_{1-x}\text{Sr}_x\text{TiO}_3$ at a doping of $x = 6\%$ (circles)¹⁵. The parameters of the calculation were $\bar{U} = 4\text{eV}$ and $J = 0.6\text{eV}$ and a reciprocal temperature $\beta = 100 \text{ eV}^{-1}$.

A comparison with the experiment is done in figure 4 using the spectrum of the orthorhombic system. The bandwidth, maximum and center of mass of the lower Hubbard band are in fair agreement with experiment. The many-body resonance at the Fermi level in the spectrum in figure 2 manifests itself as an additional structure at the Fermi level as a consequence of the convolution with the Fermi function. Note that such a structure – although less pronounced – can be seen in the experimental data, too. There are, of course, still differences in the exact distribution of the spectral weight between experiment and our theory, which possibly originate from our approximation of a purely local self-energy. Nevertheless, compared to the pure LDA result, which gives a completely wrong account of the spectrum, the LDA+DMFT appears to capture the essentials of the physics in this material.

IV. SUMMARY

In this paper we have described one possible realization of a combination of density-functional theory with the LDA approximation and the recently developed dynamical mean field theory to obtain a first-principles calculation scheme for strongly correlated electron systems. To solve the DMFT equations we used the Non-Crossing approximation, which allowed us to include all local Coulomb interactions in our calculations, which is important to reproduce the full multiplet structure in the atomic limit. In order to test the method, we showed results for the doped Mott-Hubbard insulator $\text{La}_{1-x}\text{Sr}_x\text{TiO}_3$. The comparison of our results with a photoemission experiment shows, that the lower Hubbard band is of the correct width and the center of mass of both experiment and theory is at the same position. Also, a shoulder seen at the Fermi energy in experiment is accounted for by our results as the onset of a many-body resonance. In addition, the method appears to be very sensitive to the atomic parameters and is clearly able to discriminate between different crystal structures and symmetries, although the lattice enters the DMFT only in an averaged manner. In total the results are very encouraging for the perspective of future applications.

ACKNOWLEDGEMENTS

This work was partially supported by the DFG grant PR 289/5/1&2.

- ⁹ H. Keiter, J. C. Kimbal, Phys. Rev. Lett. **25**, 672 (1970); N. E. Bickers, D. L. Cox, J. W. Wilkins, Phys. Rev. B **36**, 2036 (1987).
- ¹⁰ K. Held, D. Vollhardt, Euro. Phys. J. B **5**, 473 (1998).
- ¹¹ O. K. Andersen, Phys. Rev. B **12**, 3060 (1975); O. Gunnarsson, O. Jepsen, O. K. Andersen, Phys. Rev. B **27**, 7144 (1983).
- ¹² O. Gunnarsson, O. K. Andersen, O. Jepsen, J. Zaanen, Phys. Rev. B **39**, 1708 (1989).
- ¹³ I. Solovyev, N. Hamada, K. Terakura, Phys. Rev. B **53**, 7158 (1996).
- ¹⁴ W.E.Pickett, S.C.Erwin, E.C.Ethridge, Phys. Rev. B **58**, 1201 (1998).
- ¹⁵ A. Fujimori, et al., Phys. Rev. B **46**, 9841 (1992). (Actually, in this article, the chemical formula of the sample was $\text{LaTiO}_{3.03}$, but the excess of oxygen produces 6% holes, which is equivalent to doping with 6% Sr.)
- ¹⁶ A. C. Hewson: The Kondo Problem to Heavy Fermions, Cambridge University Press, Cambridge (1993).

- ¹ P. Hohenberg, W. Kohn, Phys. Rev. **136**, B864 (1964); W. Kohn, L. J. Sham, Phys. Rev. **140**, A1133 (1965).
- ² V. I. Anisimov, J. Zaanen, O. K. Andersen, Phys. Rev. B **44**, 943 (1991).
- ³ V. I. Anisimov, F. Aryasetiawan, A. I. Lichtenstein, J. Phys.: Condens. Matter **9**, 767 (1997).
- ⁴ V. I. Anisimov, A. I. Poteryaev, M. A. Korotin, A. O. Anokin, G. Kotliar, J. Phys.: Cond. Matter **9**, 7359 (1997).
- ⁵ Th. Pruschke, M. Jarrell and J. K. Freericks, Adv. in Phys. **44**, 187 (1995); A. Georges, G. Kotliar W. Krauth, M. J. Rozenberg, Rev. Mod. Phys. **68**, 13 (1996).
- ⁶ M. Jarrell, Phys. Rev. Lett. **69**, 168 (1992); M. Rozenberg, X. Y. Zhang, G. Kotliar, Phys. Rev. Lett. **69**, 1236 (1992); A. Georges, W. Krauth, Phys. Rev. Lett. **69**, 1240 (1992).
- ⁷ M. Caffarel, W. Krauth, Phys. Rev. Lett. **72**, 1545 (1994); M. Rozenberg, G. Moeller, G. Kotliar, Mod. Phys. Lett. B **8**, 535 (1994); Q. Si, M. Rozenberg, G. Kotliar, A. E. Ruckenstein, Phys. Rev. Lett. **72**, 2761 (1994).
- ⁸ A. Georges, G. Kotliar, Phys. Rev. B **45**, 6479 (1992).